J Paleolimnol (2020) 63:305–322
https://doi.org/10.1007/s10933-020-00117-1

ORIGINAL PAPER

Magnetic fabrics preserved by post-glacial sediment in two New York Finger Lakes (USA) revealed evidence for deformation during coring and an erosional unconformity

Tara M. Curtin · Megan L. Crocker · Gwendolyn Wheatley

Received: 13 April 2019 / Accepted: 29 February 2020 / Published online: 11 March 2020

Abstract The oceanographic community routinely uses anisotropy of magnetic susceptibility to identify deformation associated with sediment core collection and sampling, as well as to reconstruct primary and post-depositional conditions. These measurements are also applicable to lacustrine settings. Using anisotropy of magnetic susceptibility, in combination with geochemical and physical analyses of lake sediments, permits differentiation of primary depositional conditions from sediment disturbance associated with post-depositional processes and core collection. Detailed analysis of piston cores from Seneca Lake and Owasco Lake, New York (USA) revealed evidence for relatively weak anisotropies that resulted from normal lacustrine sedimentation since ~ 16.8–16.6 cal ka BP. A middle to late Holocene lowstand and associated erosional unconformity was inferred in both lakes using the magnitude of the anisotropy, changes in lithofacies, and increase in % sand. Anomalous magnetic fabrics were also preserved in post-glacial sediment that resulted from core collection and subaqueous slides. Stratigraphic disruptions ("flow-ins") that formed during coring were recognized by vertically oriented laminae or soupy sediment near the base and top of cores, respectively, and confirmed the rationale for using magnetic fabric measurements. Mid-core "flow-ins" throughout the uppermost 1–2 m of three of the four cores in this study could only be identified by a gradual shift in the dominant shape of the magnetic fabric. Imperfect piston coring likely resulted in vertical strain that produced overthickened sections without destroying the stratigraphic integrity of these sediments. Subaqueous slides were recognized in Owasco Lake by abrupt changes in lithofacies and magnetic fabric. Anisotropy of magnetic susceptibility proved to be a powerful tool to assess lacustrine core integrity in massive and laminated sediment prior to paleoenvironmental reconstruction.

Keywords Anisotropy of magnetic susceptibility · Lake sediment · Finger lakes · Piston core · Lake level · Post-glacial

Electronic supplementary material The online version of this article (https://doi.org/10.1007/s10933-020-00117-1) contains supplementary material, which is available to authorized users.

T. M. Curtin (✉) · M. L. Crocker · G. Wheatley
Department of Geoscience, Hobart and William Smith Colleges, Geneva, NY 14456, USA
e-mail: curtin@hws.edu

M. L. Crocker
e-mail: meganlynncrocker@gmail.com

G. Wheatley
e-mail: wheatley.gwen@gmail.com

Present Address:
M. L. Crocker
Oklahoma City, OK, USA

Present Address:
G. Wheatley
Rochester, NY, USA

Introduction

Paleolimnologists routinely measure the bulk magnetic susceptibility (MS) of lake sediments, but few utilize the anisotropy of magnetic susceptibility (AMS) of the sediments to discern information about past environmental conditions (Sandgren and Snowball 2001; Schneider et al. 2004; St-Onge et al. 2008). The AMS, or the magnetic fabric, is a quantitative measure of the bulk orientation of all the grains in the sediment and can be used as a proxy for the sedimentary fabric that results during deposition and any subsequent deformation (Rees 1965; Taira and Lienert 1979). To date, most AMS investigations of lacustrine sediments have been conducted to identify whether sediment disturbance occurred during coring (Rosenbaum et al. 2000; Demory et al. 2005; Frank 2007) or sampling (Copons et al. 1997). In contrast, AMS analysis of ocean sediments is used frequently to assess not only core and sample integrity (Thouveny et al. 2000), but also to infer primary depositional conditions such as settling of grains through the water column (Rees and Woodall 1975; Tarling and Hrouda 1993) and fluctuations in the speed and direction of bottom currents (Rees 1961, 1965) in addition to post-depositional features such as bioturbation (Kent and Lowrie 1975; Ellwood 1984), soft-sediment deformation (Cronin et al. 2001; Schwehr and Tauxe 2003), and unconformities (Schwehr et al. 2006). These published laboratory and field studies established characteristic AMS signatures for depositional and post-depositional fabrics in ocean settings and provide a framework for interpreting the magnetic fabrics preserved by lacustrine sediments.

The purpose of this study was to test the applicability of using AMS to assess core integrity and infer post-glacial environmental conditions by analyzing piston cores collected from Seneca Lake and Owasco Lake, New York (USA) (Fig. 1). These Finger Lakes were selected for study because (1) high-frequency seismic reflection profile surveys exist for Seneca Lake (Halfman and Herrick 1998) and Owasco Lake (Mullins and Halfman 2001), enabling careful selection of core sites; (2) a chronology for each lake basin was already established (Dwyer et al. 1996; Wellner and Dwyer 1996; Anderson et al. 1997; Guiles-Ellis et al. 2004); (3) detailed rock magnetic analysis of Seneca Lake sediment revealed that the dominant ferromagnetic mineral is detrital magnetite (King et al. 1982); and (4) analysis of seismic reflection profiles and sediment cores revealed several primary and secondary sedimentary features, including rhythmic sedimentation, subaqueous slides, and erosional surfaces (Woodrow et al. 1969; Halfman and Herrick 1998; Mullins and Halfman 2001). Mullins and Halfman (2001) hypothesized that lowstands were responsible for the subaqueous slides and either a lowstand or an increase in the speed of lake bottom currents was responsible for the middle to late Holocene erosional surface. AMS analyses enabled us to not only test this hypothesis, but also to assess whether these analyses can be used in these lakes to distinguish primary and secondary sedimentary fabrics from coring artefacts, based on the unique AMS signatures documented for these fabrics in ocean sediments.

AMS analyses were supplemented with visual observations, petrographic analyses, geochemical analyses [loss-on-ignition (LOI)], X-ray diffraction (XRD), and grain size analyses, to bolster paleoenvironmental interpretations and infer changes in depositional and post-depositional conditions in Seneca Lake and Owasco Lake since $\sim$ 16.8–16.6 cal ka BP. Our study shows that magnetic fabric and physical and geochemical analyses can be used in concert to recognize sediment disturbance during mass movements, coring, and subsampling, as well as to identify an erosional unconformity that formed during a lake lowstand.

Study sites

Seneca Lake and Owasco Lake occupy north–south-oriented basins that originated as pre-glacial stream valleys and were widened and deepened by ice and subglacial meltwater (Mullins et al. 1996). Both lakes have symmetrical, steep, bedrock-bounded walls that extend down to a flat basin floor. A thick veneer of late Quaternary calcareous glacial drift and glacio-lacustrine deposits covers Devonian sedimentary bedrock (Mullins et al. 1996). The lake basins are filled with up to 275 m of late Quaternary sediment and < 10 m of post-glacial sediment (Mullins et al. 1996). Profundal piston cores collected from Seneca Lake reveal pink and gray proglacial varves, overlain by proglacial massive gray clay and post-glacial rhythmites (Anderson et al. 1997; Guiles-Ellis et al. 2004). The contact between proglacial and post-glacial sediment

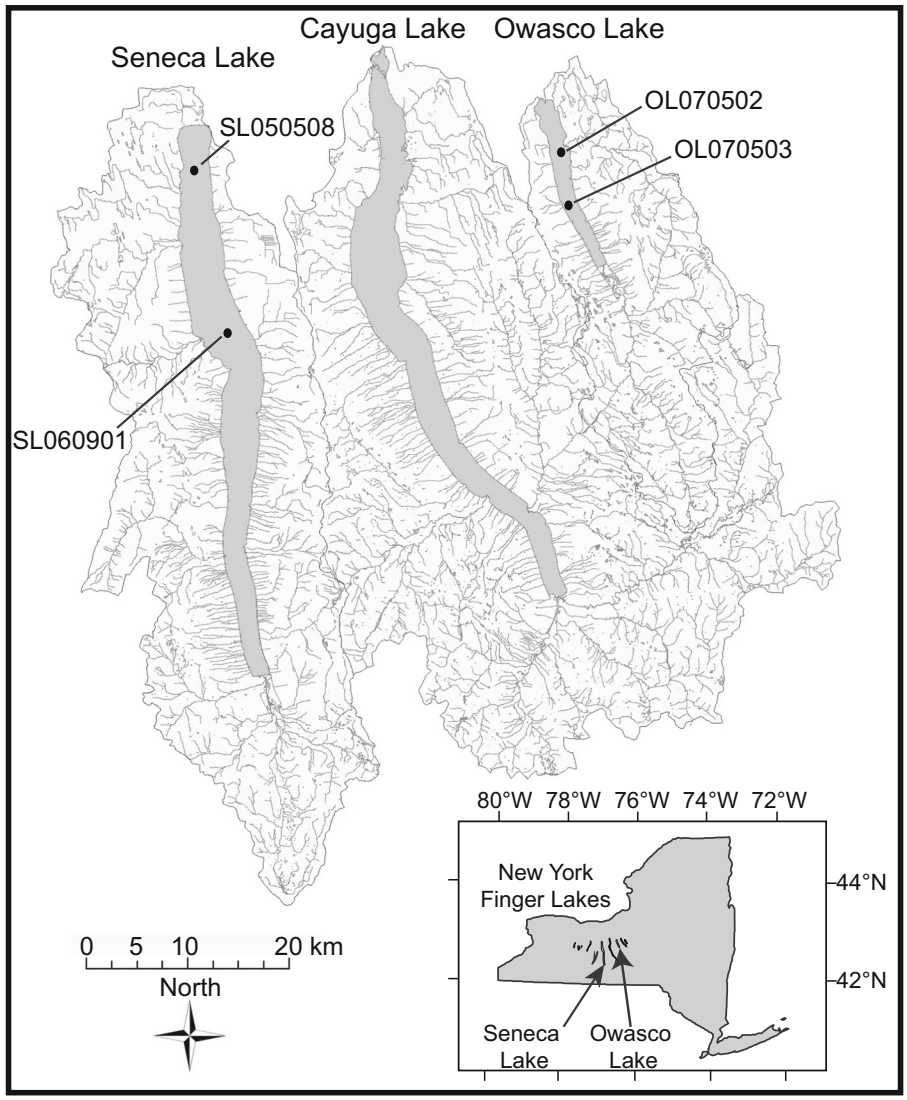

Fig. 1 Location of core sites (filled circles) in Seneca and Owasco Lakes. For each lake, the watershed is delineated and tributaries are drawn. The inset map shows the location of Seneca Lake and Owasco Lake within New York State. Core site attributes are given in the captions for Figs. 2 and 3 for Seneca Lake and Figs. 4 and 5 for Owasco Lake

in both lake basins occurs at ∼ 16.8–16.6 cal ka BP (Mullins et al. 1996; Dwyer et al. 1996). Post-glacial lacustrine sediment is comprised of marl in the littoral zone and laminated to massive predominantly siliciclastic sediment in the profundal zone (Woodrow et al. 1969; Dwyer et al. 1996; Mullins et al. 1996).

Seneca Lake [surface area (SA) = 175.4 km^2, z_{max} = 186 m, basin SA = 1181 km^2, volume = 15.54 km^3] is monomictic, and mixes during winter and spring (Schaffner and Oglesby 1978). Owasco Lake (SA = 26.7 km^2, z_{max} = 54 m, basin SA = 470 km^2, volume = 0.781 km^3) is dimictic, and mixes during spring and autumn. The water column of both lakes is oxygenated year-round (Schaffner and Oglesby 1978). Seneca Lake has a longer water residence time (12–23 years) than Owasco Lake (1.5–3 years) (Michel and Kraemer 1995). Approximately 75% of water inflow is supplied by spring snowmelt (Michel and Kraemer 1995). These lakes experience long, snowy winters and warm, humid summers (Schaffner and Oglesby 1978).

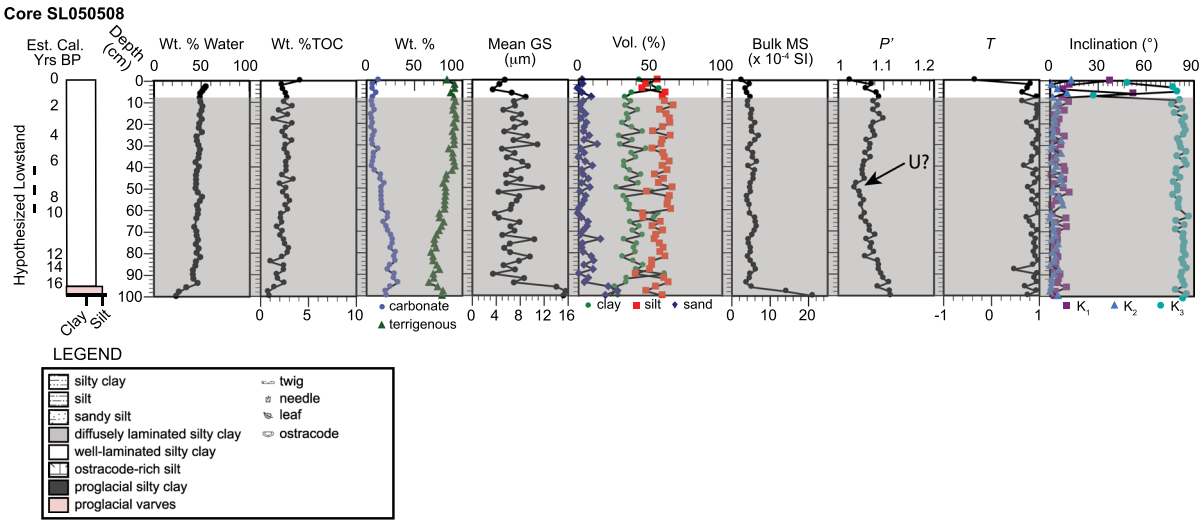

Fig. 2 Stratigraphy; % water; loss-on-ignition (%TOC, % Carbonate, % Terrigenous); mean grain size (GS); volume (Vol.) % sand, silt and clay; bulk magnetic susceptibility (MS); and magnetic fabric data (P', T, inclinations of the K_1, K_2, and K_3 axes) for core SL050508 (Lat. 42°49.578′ N, Long. 76°57.372′ W, z = 47 m, core length = 100 cm). The duration of the hypothesized lake lowstand is shown using a dashed line. Arrow points to inferred unconformity (U?) on the P' panel. The light gray box across the panels highlights sediment that preserves primary sedimentary deposition based on T values. Legend is the same for Figs. 2, 3, 4 and 5

Materials and methods

Core collection and description

One core was collected in the profundal zone from each lake to investigate a stratigraphic record with well-preserved post-glacial rhythmites and no known stratigraphic hiatuses (core SL060901 in Seneca Lake and core OL070502 in Owasco Lake). One core was also collected from a shallower site to examine an erosional surface in Seneca Lake (core SL050508) and subaqueous slides in Owasco Lake (core OL070503). Cores were collected using modified Kullenberg piston corers (Kelts et al. 1986) with a 4.0-cm diameter (Seneca Lake) and 6.5-cm diameter (Owasco Lake) (Figs. 1, 2, 3, 4, 5 provide site attributes). The corers are single-drive, cable-deployed piston corers with 6-m-long core barrels that were lined with polycarbonate plastic tubes. The corers were lowered using a winch from the coring platform, a 19.8-m-long steel-hulled vessel in Seneca Lake and a 7.6-m-long pontoon boat in Owasco Lake, until the trigger weight reached the sediment–water interface. Once triggered, the corers were released on a freefall descent to the lake bottom. Upon recovery on-board, the ends of the plastic tube were sealed with tightly fitting caps taped to the liner. Cores were stored in the dark at 4 °C and sub-sampled within 24 h of collection. Cores were split longitudinally and then separated using fishing line. Split core surfaces were lightly scraped for digital photography and visual core description. Lithofacies were defined based on macroscopic and smear-slide analysis of color, texture, sedimentary structures, composition, and subfossils of the sediment. One half of the split core was subsampled for magnetic susceptibility measurements and the other half was used for all other analyses.

Magnetic susceptibility measurements

A total of 713 samples for MS and AMS analyses were collected by pushing plastic 2 × 2 × 2 cm cubes into the center of the wet sediment of the split core surface to minimize the effect of core edge distortion. Because sample shape has been shown to be critical for AMS analyses, special care was taken to ensure cubes were completely filled with sediment (Ellwood 1979). Samples were stored at 4 °C in the dark when not being measured, to minimize desiccation and oxidation. Measurements of magnetic low field bulk susceptibility and AMS were performed using a Kappabridge KLY-4S in a field intensity of

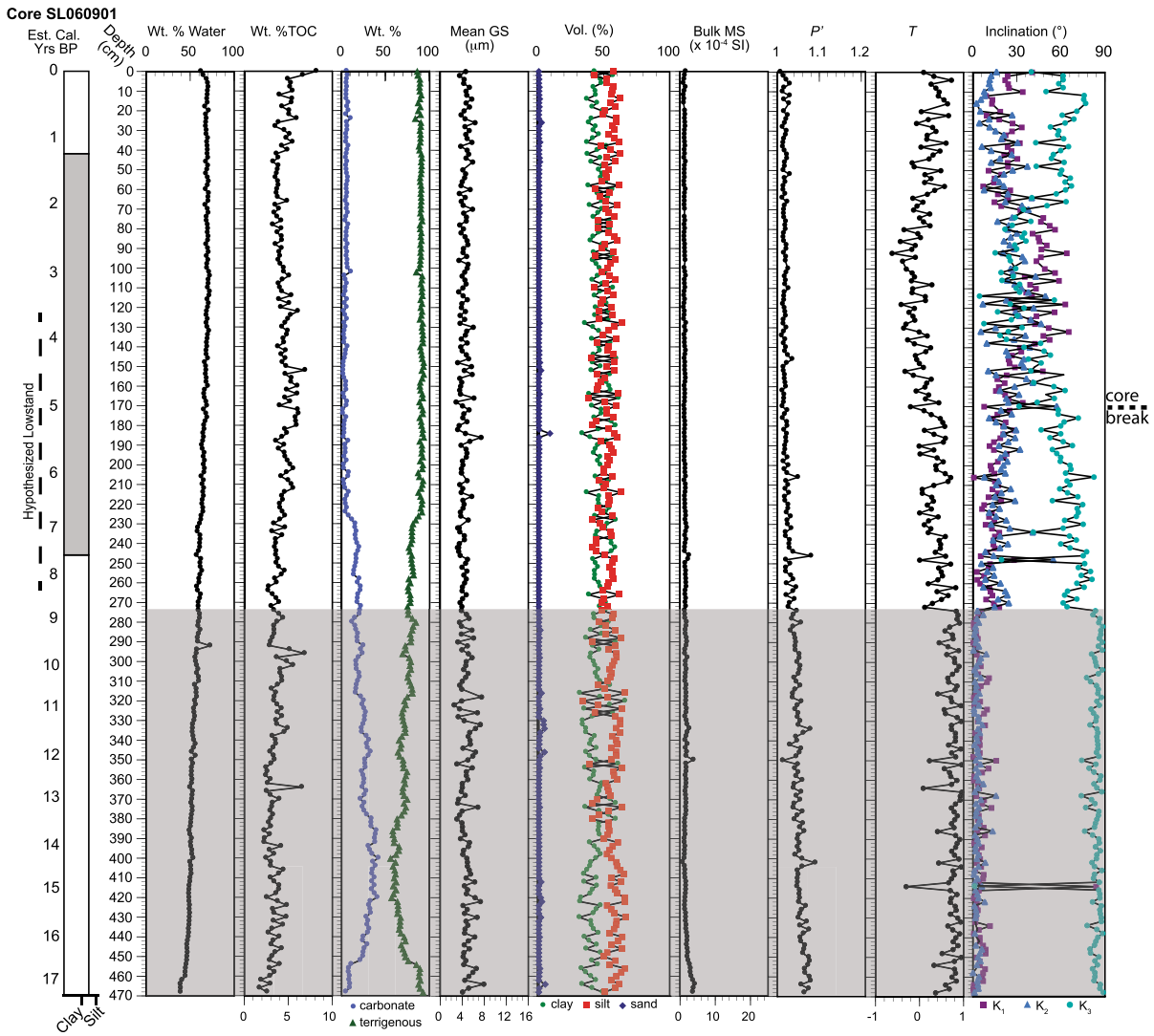

Fig. 3 As Fig. 2, but for core SL060901 (Lat. 42°41.453′ N, Long. 76°55.093′ W, z = 148 m, core length = 468 cm). The dashed line on the right-hand side of the figure marks the position of the core liner break

300 A m^{-1}. Bulk MS was measured to estimate the contribution of magnetic particles in the sediment. AMS measurements were made using the fifteen directional susceptibilities scheme of Jelinek (1978) in triplicate, and averages were reported. AMS quantifies the induced, combined magnetic contributions of the ferromagnetic (i.e. magnetite, hematite), paramagnetic (i.e. micas, clays) and diamagnetic (i.e. quartz, feldspar, calcite) grains in each sample (Tarling and Hrouda 1993). Results of AMS analyses show the bulk orientation of all mineral grains in a sample, and are represented in three-dimensional space by an ellipsoid. The three axes of the magnetic ellipsoid correspond to the maximum (K_1), intermediate (K_2), and minimum (K_3) principal axes (Tarling and Hrouda 1993). The ellipsoid represents the combined results of the AMS produced by individual grain shape, composition, and crystallography in addition to grain alignment in each sample. MS is dimensionless and expressed in SI units.

The corrected degree of anisotropy of the resulting ellipsoid (P') and the ellipsoid shape factor (T) were used to evaluate the magnetic fabric (Ellwood et al. 1988). The Kappabridge software, *Sufar v. 1.2*, determines the anisotropy tensor as represented by K_1, K_2, and K_3, as well as their representative

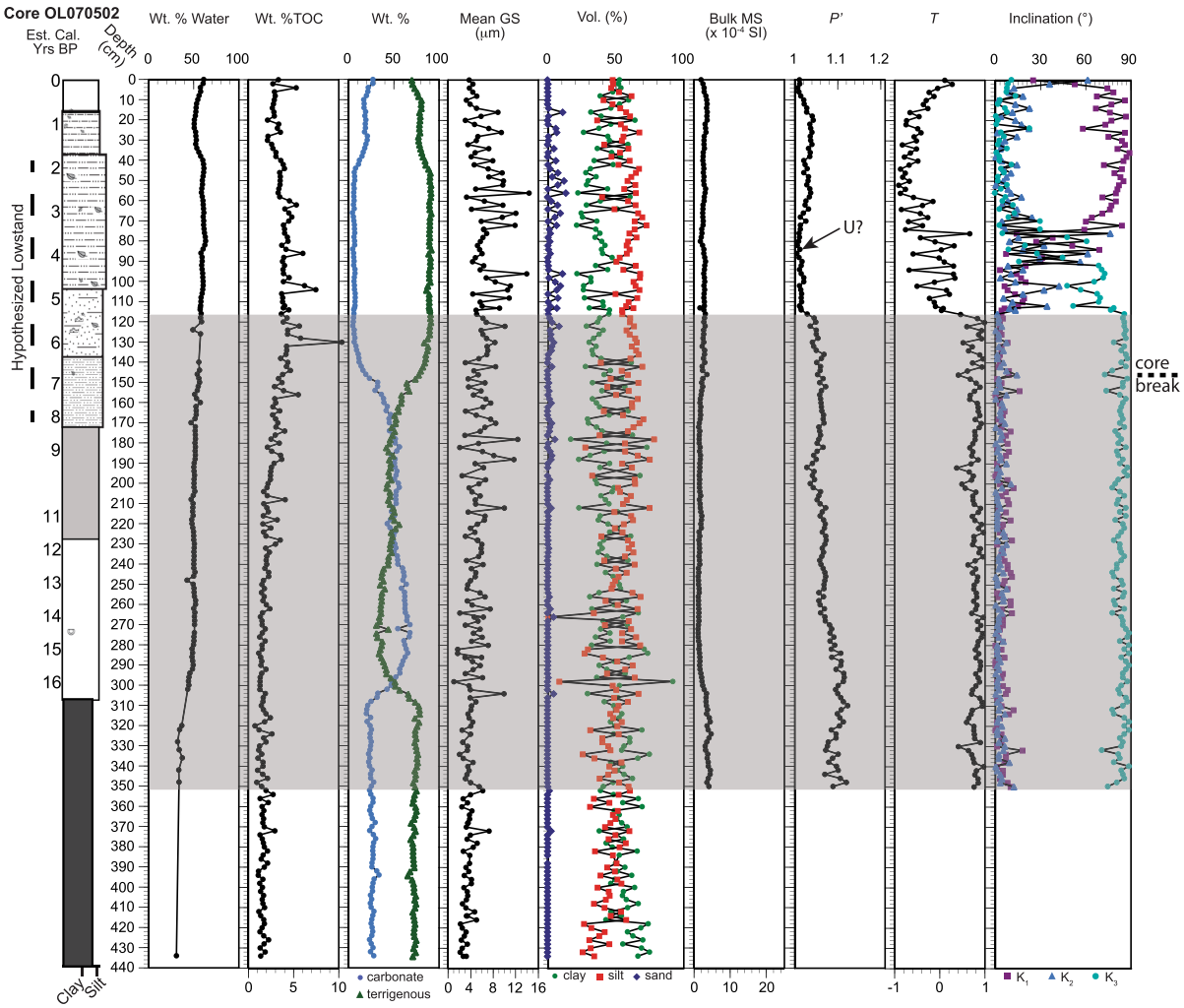

Fig. 4 As Fig. 2, but for core OL070502 (Lat. 42°52.962′ N, Long. 76°31.550′ W, z = 33 m, core length = 431 cm). The dashed line on the right-hand side of the figure marks the position of the core liner break

orientation angles. Orientation angles are given with respect to sample coordinates because the samples are only semi-oriented. During coring, the core barrel rotates, which does not permit sampling for AMS with known geographic coordinates. The software also calculates the magnetic anisotropy factors P' and T. The parameter, P', is defined as:

$$P' = \exp\left\{2\left[(\eta_1 - \eta_m)^2 + (\eta_2 - \eta_m)^2 + (\eta_3 - \eta_m)^2\right]\right\}^{1/2} \quad (1)$$

(Jelinek 1981)

where $\eta_1 = \ln K_1$, $\eta_2 = \ln K_2$, $\eta_3 = \ln K_3$ and $\eta_m = (\eta_1\eta_2\eta_3)/3$ and $K_1 > K_2 > K_3$ are the principal susceptibilities in SI units. P' mathematically represents the degree of anisotropy of the resulting magnetic ellipsoid. Greater P' values reflect a more developed magnetic anisotropy (Tarling and Hrouda 1993). Replicate analyses of each sample resulted in P' values within 0.002. The shape parameter, T, is defined as:

$$T = (2\eta_2 - \eta_1 - \eta_3)/(\eta_1 - \eta_3) \quad (2)$$

(Jelinek 1981).

When $0 < T \leq 1$, then the ellipsoid is oblate, whereas if $-1 \leq T < 0$, the ellipsoid is prolate (Tarling and Hrouda 1993). The shape of the ellipsoid and orientation of principal axes provide information about primary sediment deposition and post-

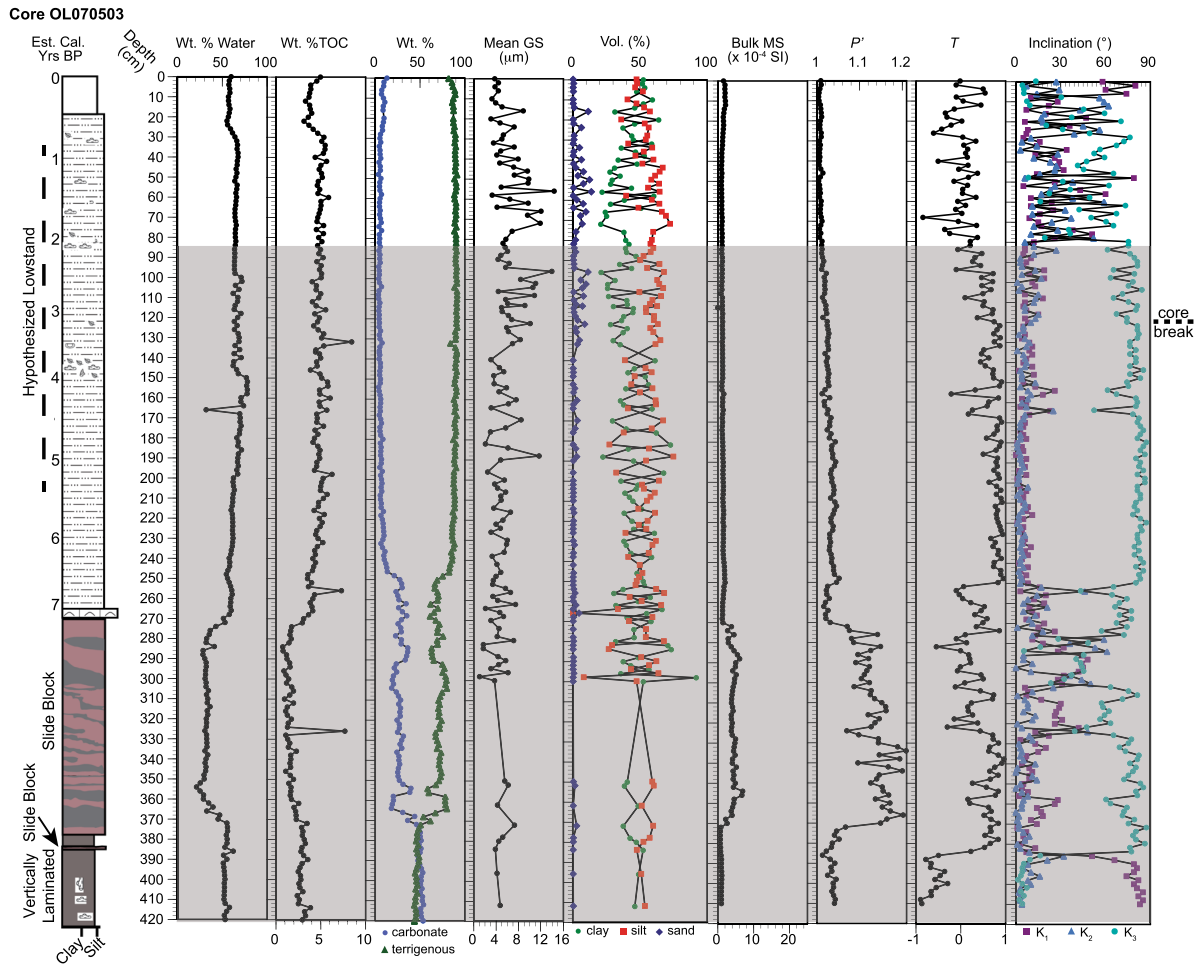

Fig. 5 As Fig. 2, but for core OL070503 (Lat. 42°48.900′ N, Long. 76°30.280′ W, z = 50 m, core length = 410 cm). Two subaqueous slides occur near the bottom third of the core. Vertically laminated sediment occurs at the base. The dashed line on the right-hand side of the figure marks the position of the core liner break

depositional deformation. An oblate shape is typical for sediment that accumulates in relatively quiet to moderately fast-moving currents (Tarling and Hrouda 1993). A prolate shape may reflect primary deposition if currents are strong enough to orient grains perpendicular to the main flow direction or deformation of the sedimentary fabric during post-deposition or sampling (Kent and Lowrie 1975; Tarling and Hrouda 1993; Copons et al. 1997). Deformation during coring may produce an increased dispersion and lower average inclination of K_3 axes (Rosenbaum et al. 2000). Sampling-induced fabrics typically produce E–W trending K_1 and/or N–S trending K_3 axes in geographic coordinates (Copons et al. 1997; Aubourg and Oufi 1999). The orientation of the principal axes in sample coordinates were plotted on stereonets to test for these possibilities.

Petrographic analysis

Sediment slabs were collected from representative core segments with anomalous (prolate) and typical (oblate) AMS fabrics from core SL060901. Slabs were impregnated with low-viscosity Spurr Resin, and prepared as thin-sections for petrographic analysis (Lamoureux 1994).

Physical and geochemical analyses

Contiguous subsamples from each core were collected at 2-cm intervals, weighed, frozen, freeze-dried, and

reweighed to determine the weight percent water content. Freeze-dried samples were homogenized for physical and geochemical analyses. Terrigenous particle size was measured to assess relative depositional energy. Prior to grain-size analysis using a Beckman Coulter LS230 Multivariable Laser Diffraction Particle Size Analyzer, subsamples were treated with 30% hydrogen peroxide to remove organic matter and with 25% glacial acetic acid to remove calcium carbonate, following the methods of Jackson (1969). These components were assumed to be autochthonous based on Effler et al. (1987) and Meyers (2002), and were removed to isolate terrigenous sediments.

Samples were analyzed in duplicate for percent organic carbon by weight (%TOC) and calcium carbonate content by weight (%TC) by sequential LOI at 550 °C (4 h) and 1000 °C (2 h), respectively (Dean 1974), and means were reported. The %TOC was estimated by dividing the mass difference between the freeze-dried sample and the mass after ashing at 550 °C by the weight of the freeze-dried sample. This value was divided by 2.13 because the %TOC is about twice the organic matter content (Dean 1974). The %TC was calculated by multiplying the weight loss after combustion at 1000 °C by 2.274 (the ratio of the molecular weight of $CaCO_3$ and CO_2). The %TOC values provide insight on biomass production and preservation in the lakes. The %TC values were used to correlate cores collected from Seneca Lake using the methods of Guiles-Ellis et al. (2004).

The mineralogy of powdered samples subsampled at 2-cm intervals from core SL050508 was determined by XRD using a Rigaku Multiflex. Samples were crushed using an agate mortar and pestle, sieved, and micronized in isopropyl alcohol for 7 min. Ground samples were side-loaded into an aluminum sample holder to retain random orientation**.** Samples were scanned from 5° to 65° 2θ using a step size of 0.02° 2θ and a 1 s count time. Semi-quantitative mineral abundances were calculated using the area of selected peaks and mineral intensity factors from Hoffman (1976) and Bayliss (1986).

Chronology

Temporal control of sediment cores from Seneca Lake and Owasco Lake was established using previously published radiocarbon ages that were calibrated using CALIB version 7.1 (Reimer et al. 2009). Anderson et al. (1997) and Guiles-Ellis et al. (2004) reported radiocarbon dates for bulk organic matter samples from Seneca Lake where changes in the %TC of the post-glacial sediment are significant. Radiocarbon dates for aquatic organic macrofossils and peats reported by Dwyer et al. (1996) and Wellner and Dwyer (1996) were used to constrain the ages of cores from Owasco Lake. We assigned approximate ages in thousands of calendar years before present (cal ka BP) to Seneca Lake cores in this study by correlating the %TC contents and by changes in lithology in Owasco Lake cores [Electronic Supplementary Material (ESM) Tables S1 and S2]. We did not apply a correction factor to the published ages because Wellner and Dwyer (1996) verified the radiocarbon ages of peats using paleomagnetic secular variations and found no evidence for significant reservoir or hardwater effects.

Results

Five post-glacial lithofacies were recognized: (1) rhythmically laminated silty clay, (2) massive silty clay, (3) ostracode-rich silt, (4) vertically laminated "flow-in" sediments, and (5) contorted beds of pink and gray proglacial varves (Figs. 2, 3, 4, 5). Cores collected from Seneca Lake preserve only rhythmically laminated silty clay, whereas collectively, cores from Owasco Lake record all five lithofacies. Results of LOI, grain size, MS, and AMS analysis of these lithofacies are described below for each lake.

Seneca Lake

Cores SL050508 and SL060901 bottom out in pink and gray, organic-poor, carbonate-rich, bedded proglacial varves and massive gray clay (not discussed here) and preserve the same post-glacial lithofacies: rhythmically laminated olive-gray and black silty clay (Figs. 2, 3). Although in core SL050508 there is no systematic pattern, laminae thickness changes drastically from cm- to mm-scale throughout core SL060901, with more abundant, thicker black laminae near the base (468–272 cm) and top of the sequence (50–0 cm) and diffuse laminae in the middle section (272–50 cm). Olive-gray laminae are massive or fine upwards and are composed of siliciclastic minerals, calcite, and organic matter (ESM Fig. S1A). Organic

matter drapes the olive-gray laminae. Diffusely laminated sections preserve peloids and burrows (ESM Fig. S1B).

In both cores, the % water gradually increases upcore. The %TC exhibits an abrupt rise from ~ 5 to ~ 32–42% and then a gradual stepwise decline back to ~ 5% proceeding to the top of both cores. The %TOC gradually rises from ~ 1 to 2% at the base of the cores to ~ 4–10%, and then back to ~ 1–3% except near the core top where the %TOC is greatest (4–8%). This lithofacies is mainly comprised of siliciclastic sediment (> 65%). The mean grain size, % sand, and bulk MS are highest near the base of the lithofacies and, in general, decrease upcore. XRD analysis of core SL050508 complements LOI results and demonstrates that quartz and calcite are the dominant components of the sediment (ESM Fig. S2A). Clay mineral abundance increases from ~ 1.5% at the base to ~ 7–13% at the top of core SL050508 (ESM Fig. S2B).

There are striking differences in the AMS of both cores. The AMS for core SL050508 corresponds to an oblate fabric, except at the core top. In core SL060901, T systematically decreases upcore from 0.94 (oblate) to -0.63 (prolate) and then increases again to 0.98 (oblate). At the core top, T is negative (prolate). The inclination of the K_1, K_2, and K_3 axes reflect these differences in T. Except for the core top of SL050508, K_1 and K_2 are subparallel to bedding and K_3 is close to vertical. In contrast, K_1, K_2, and K_3 for core SL060901 range widely. When laminae are well-developed, K_3 approaches vertical (~ 73°–87°) and K_1 and K_2 are similar to each other and subparallel to bedding (~ 0.7°–22°). In the diffusely and well-laminated sequence, where T is negative, K_3 is significantly lower, ~ 30°, and K_1 and K_2 approach 60°. Overall, P' is very low in both cores. However, trends in P' are quite different. In core SL050508, P' is greatest near the base of the lithofacies (1.11) and gradually decreases (to 1.03) by 50 cm depth and then increases towards the top of the core (1.08). In core SL060901, P' generally decreases upcore, from 1.07 to 1.01.

Both cores span the entire Holocene although core SL050508 appears to preserve a condensed sedimentary sequence. The rapid change in P' in core SL050508 occurs at ~ 7 cal ka BP. Prolate fabrics in core SL060901 occur between ~ 7 and ~ 2 cal ka BP, and coincide with both diffusely and well-laminated rhythmites.

Owasco Lake

Collectively, the Owasco Lake cores preserve all five lithofacies, but the two most prevalent are massive silt and diffusely to well-laminated olive-gray and black silty clay. Core OL070502 bottoms out in proglacial massive gray clay (432–310 cm, not discussed here) and is overlain by two postglacial lithofacies: well-laminated olive-gray and black silty clay (310–230 cm), very dark to light gray massive silt (230–17 cm) and well-laminated olive-gray and black silty clay (17–0 cm) (Fig. 4). In contrast, Core OL070503 bottoms out in visibly disturbed, vertically ("flow-in") laminated olive-gray and black sediment with twigs (422–402 cm) overlain by diffusely horizontally laminated olive-gray and black silty clay (398–274.5 cm) interbedded with two intervals of chaotically laminated pink and gray, organic-poor, carbonate-rich proglacial varves (389–388 cm, 371–275 cm) followed by ostracode-rich silt (274.5–271 cm), very dark to light gray massive silt (271–17 cm) and well-laminated olive-gray and black silty clay (17–0 cm) (Fig. 5).

These post-glacial lithofacies have unique sediment compositions and magnetic fabrics. The two beds of pink and gray proglacial varves in core OL070503 that display internal soft-sediment deformation are comprised of carbonate (20–30%) and terrigenous sediment (70–80%), are fine-grained (average 2–7 μm), and have the lowest water content (~ 30%) and highest bulk MS (2 to 7 × 10^{-4} SI units) and P' (1.12–1.20) compared to all other lithofacies. In this lithofacies, T fluctuates, and ranges from − 0.31 (prolate) to 0.91 (oblate). The ostracode-rich silt lithofacies has a moderate water content (36–48%), low %TOC (~ 2%), higher %TC (~ 30%), even higher terrigenous content (~ 70%), moderate bulk MS (2 to 4.8 × 10^{-4} SI Units), low P' (1.071 to 1.14), and T that ranges from 0.58 to 0.86 (oblate).

The very dark to light gray massive silt lithofacies was recovered in both cores and is the dominant lithofacies. This lithofacies has a higher %TOC (6–8%), is coarser grained (average is 14.4 μm), and contains more sand (up to 13%) than the other lithofacies. It is comprised of mainly terrigenous sediment (60–90%), and little carbonate (~ 5%) and organic carbon (~ 4.5%). The water content increases upcore from 47 to 67%. The MS varies from 1.1 to 3.7 × 10^{-4} SI Units, and P' is very low (1.01–1.07).

This lithofacies is characterized by prolate magnetic ellipsoids ($T < 0$). K_1 is nearly vertical ($\sim 80°$), whereas K_2 and K_3 are subparallel to the depositional surface.

The composition and magnetic fabric of the diffusely to well-laminated olive-gray and black silty clay that occurs in both cores is very similar to that observed in Seneca Lake. The water content (33–60%), %TOC (1.2–10.3%), %TC (4–67%), and terrigenous content (30–90%) varies significantly by depth. This lithofacies is characterized by a low bulk MS (1.11 to 3.56 $\times$ 10^{-4} SI units) and P' (1.01–1.12). The diffusely laminated to massive sediment preserves an anomalous magnetic fabric, whereas the well-laminated mud preserves an oblate fabric with near vertical K_3 axes and K_1 and K_2 axes that are parallel to bedding. The "flow-in" lithofacies observed at the base of core OL070503 is similar in composition and physical characteristics as the diffusely laminated silty clay lithofacies, and preserves an anomalous magnetic fabric. T is < 0 (prolate), and K_1 is almost vertical.

Core OL070502 appears to preserve a condensed section of post-glacial sediment whereas core OL070503 preserves only the last $\sim$ 7 cal ka BP (Figs. 4, 5). Prolate magnetic fabrics in these cores do not occur simultaneously, or in the same lithofacies. In core OL070502, they occur over the last $\sim$ 6 cal ka BP and in OL070503, over the last $\sim$ 2 cal ka BP.

Fidelity of the AMS measurements

The orientations of the K_3 axes of most samples are perpendicular or nearly perpendicular to bedding, typical of a sedimentary fabric that reflects primary depositional conditions (Figs. 2, 3, 4, 5, 6). Within three of the four cores, however, there is a systematic upcore trend in both T and the inclination of the K_3 axes. The orientations of K_3 axes deviate from vertical for $\sim$ 1–2 m within the uppermost portions of three cores and T is < 0. To assess whether the samples that exhibit a prolate magnetic fabric reflect primary depositional conditions or coring or sampling-induced errors, just those samples were plotted on stereonets (ESM Fig. S3). These reveal some bias of the magnetic fabric. In each core, the K_1 axes of several samples are clustered parallel to subparallel to 90° and 270° whereas most K_2 and K_3 axes are widely scattered. There is a broad similarity in how K_1, K_2, and K_3 axes cluster in core SL060901 and core OL070502. There are several explanations that can account for anomalous magnetic fabrics, including sediment composition, mass movement, fast-moving currents, deformation during core collection, and core splitting and sampling, which are discussed below.

Discussion

The composition and fabric of the lake sediment influences its magnetic properties

Lake sediment contains minerals, rock fragments, organic matter, and subfossils that each makes its own contribution to the bulk MS and AMS (Tarling and Hrouda 1993). The low bulk MS of these cores indicates the predominance of diamagnetic and paramagnetic grains over ferromagnetic grains (Figs. 2, 3, 4, 5). XRD analysis of core SL050508 documents that most of the sediment is comprised of material sourced from the watershed, and the dominant terrigenous minerals are quartz and clay minerals (ESM Fig. S2). This source interpretation is consistent with King et al. (1982), who established that magnetite in Seneca Lake sediments was likely derived from the watershed and washed into the lake based on its coarse magnetic grain size.

The difference in the bulk MS of the beds comprised of proglacial varves versus the post-glacial lithofacies implies some compositional control. Beds comprised of proglacial varves have much higher bulk MS than the other lithofacies. The degree of erosion in the watersheds may account for this difference. Higher bulk MS in beds comprised of proglacial varves are likely the result of greater erosion rates of paramagnetic and ferromagnetic grains in the sparsely vegetated watersheds when the ice sheet was within the watersheds. Lower values in younger sediments could reflect periods of decreased erosion caused by an increase in vegetation cover. The relationship between bulk MS and sediment composition is less clear in the younger lithofacies because the relative proportion of diamagnetic and paramagnetic minerals changes.

Because there is no or a very weak inverse relationship between %TOC and % water with P' and no relationship between %TC and P', these diamagnetic materials do not appear to control the AMS (Fig. 7a–c). In these lakes, paramagnetic clay

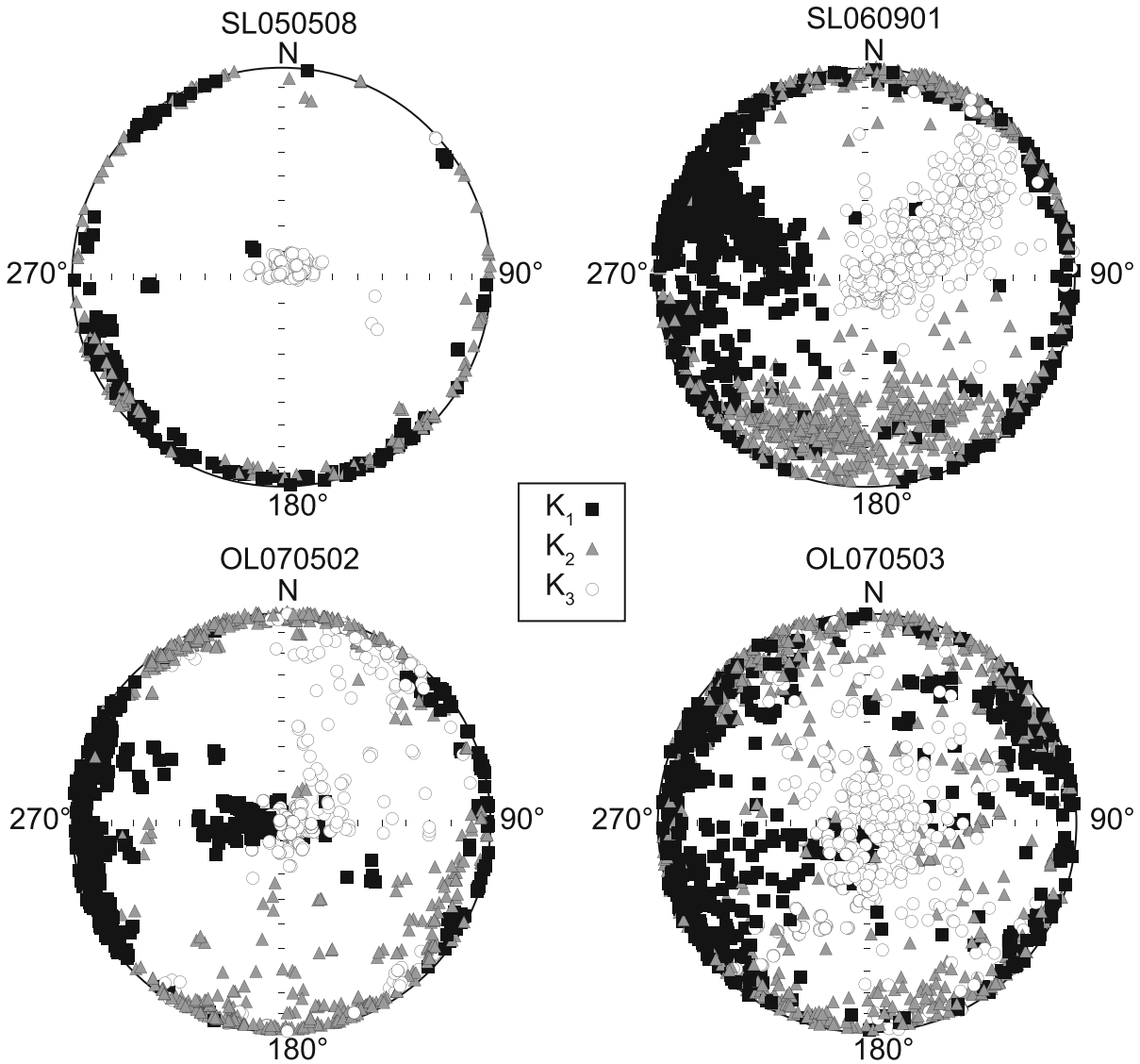

Fig. 6 Orientation of the principal axes of susceptibility are plotted in sample coordinates on an equal area stereonet for cores SL050508, SL060901, OL070502, and OL070503. Filled squares, filled triangles, and open circles represent maximum (K_1), intermediate (K_2), and minimum (K_3) axes of susceptibility, respectively

minerals likely play a more important role, similar to what is observed in other fine-grained sediments (Parés 2015). The bulk MS and P' in the two deepwater cores, SL060901 and OL070503, both show an overall decrease upcore, suggesting that either the relative proportion of clay minerals was higher near the base and decreased upcore or the alignment of platy clay minerals was greatest near the core bottoms, possibly because of compaction. The lack of a relationship between bulk MS and P' in all the cores suggests that the sediment fabric rather than the composition controls the AMS (Fig. 7d). Cores collected from shallower lake depths show more variation in bulk MS and P' and do not follow the same trend. In core SL050508 and core OL070502, the general decline in P' upcore continues until 50 cm or 100 cm, respectively, during the mid-Holocene, after which P' increases. Because bulk MS does not exhibit

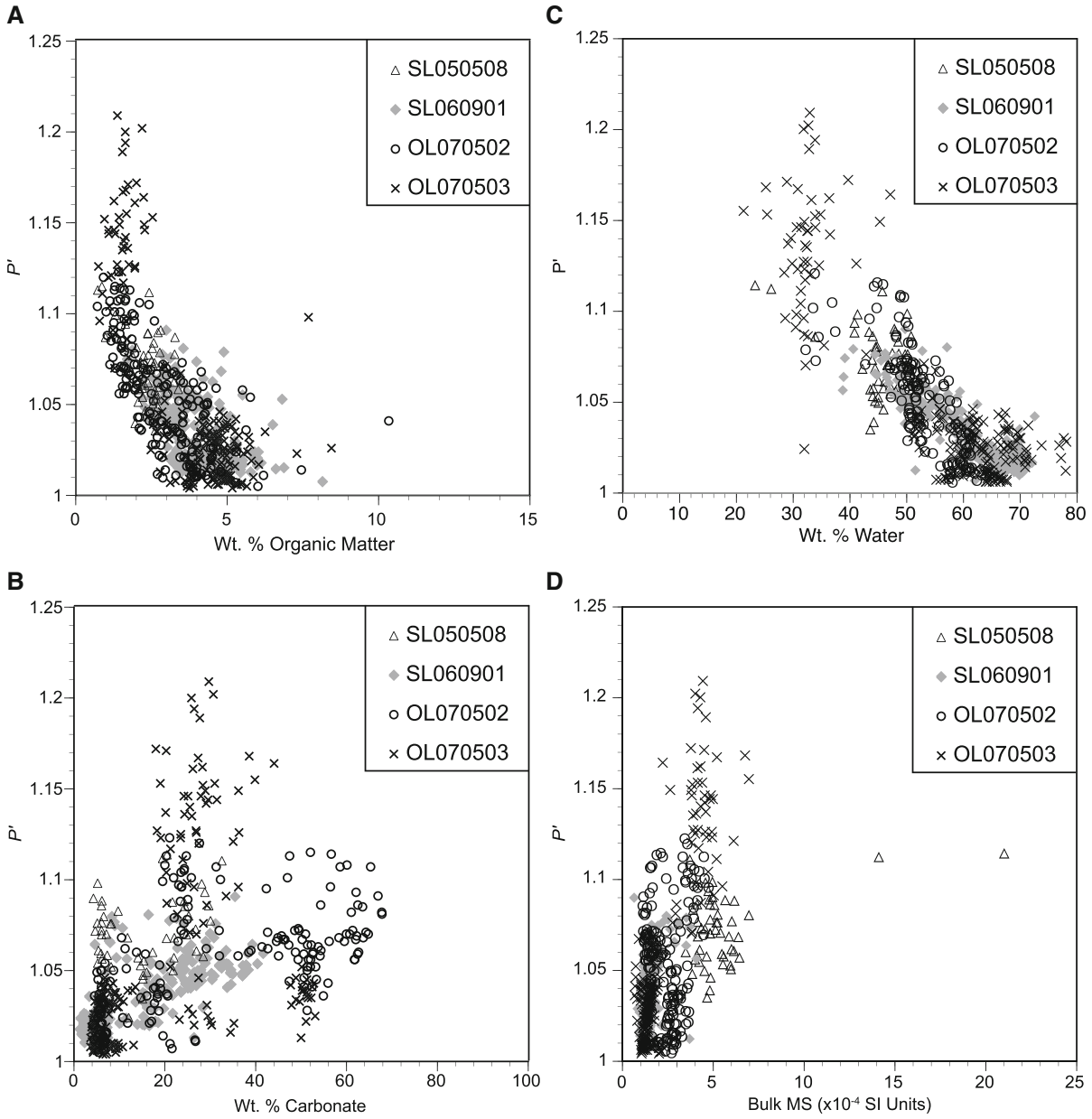

Fig. 7 **a** Weight percent (wt%) organic carbon content versus the strength of the anisotropy of magnetic susceptibility (P') for cores SL050508, SL060901, OL070502, and OL070503. **b** wt% carbonate content versus P' for cores SL050508, SL060901, OL070502, and OL070503. **c** wt% water content versus P' for cores SL050508, SL060901, OL070502, and OL070503. **d** Bulk MS versus P' for cores SL050508, SL060901, OL070502, and OL070503

the same trend as P', we infer that the degree of alignment of these platy minerals controls P', rather than a higher concentration of clay minerals. XRD analyses of SL050508 support this claim. The trend in P' does not mimic the changes in clay mineral concentrations (Fig. 2; ESM Fig. S2B).

Anomalous magnetic fabrics may be caused by slides and core collection

Interpretation of the magnetic fabric of Seneca Lake and Owasco Lake cores is based on the distribution of the orientations of the principal AMS axes. Most of the

sediment preserves K_1 axes parallel to the depositional plane and K_3 axes perpendicular to it, resulting in oblate magnetic ellipsoids (Figs. 2, 3, 4, 5). This AMS signature commonly results from gravitational and tractive forces that operate during deposition to create a preferred orientation of grains parallel to bedding (Rees 1965; Tarling and Hrouda 1993). In these lakes, the AMS is likely the result of deposition in relatively quiet to slow-moving waters, allowing alignment of sediment grains parallel to sub-parallel to the lake bottom. This is consistent with the fine-grained nature of the sediment and presence of laminae throughout much of Seneca Lake and Owasco Lake's post-glacial history. It is possible that coincident increases in mean grain size and P', when the magnetic fabric is oblate, reflect an increase in the velocity of currents in these lakes. Moderate-velocity flow conditions can result in slightly imbricated sediment grains, causing K_3 axes to deviate up to $\sim$ 20° from vertical, and even faster flow can result in prolate fabrics (Tarling and Hrouda 1993). We discounted very fast currents because core intervals with the coarsest grain size and highest % sand found in Owasco Lake often have oblate rather than the expected prolate fabrics. Although most sediment that accumulated in Seneca Lake and Owasco Lake preserves an oblate magnetic fabric, prolate fabrics occur over several meters in these cores. A combination of AMS and geochemical and physical analyses permits discrimination among these potential processes responsible for the anomalous magnetic fabrics: mass movements, bioturbation, and deformation during core collection and subsampling.

Two beds with anomalous magnetic fabrics occur near the base of core OL070503 (Fig. 5). They exhibit the same lithological and textural characteristics as the proglacial varves in Seneca Lake described by Woodrow et al. (1969). In Owasco Lake, these beds occur within younger, olive-gray laminated sediment. We infer that they are part of the middle Holocene subaqueous slide unit recognized by Mullins and Halfman (2001). Within both beds, varves are contorted, which likely resulted in the rapid changes in and wide range of the orientation of K_3 axes and variable magnetic fabrics, from prolate to oblate. Identifying mass movements in sediment cores can be challenging (Cronin et al. 2001; Schwehr et al. 2006), but because these beds have unique bulk MS, AMS, physical, and geochemical signatures, they can be distinguished from undisturbed sediment.

Visual and petrographic observations reveal that bioturbation could be responsible for prolate fabrics preserved by the diffusely laminated silty clay in core SL060901 and massive silt in core OL070502 and core OL070503 (Figs. 3, 4, 5). Peloids and vertically to subvertically oriented burrows identified in thin section occur in diffusely laminated sediment that preserves the lowest P' and T and greatest K_1 orientations in core SL060901 (Fig. 2; ESM Fig. S1B). Early experimental work suggested that bioturbation destroys any preferred grain orientation and therefore the magnetic fabric acquired during deposition (Kent and Lowrie 1975). However, more recent laboratory experiments by Katari et al. (2000) demonstrate sediment that was bioturbated, but not resuspended, showed no change in magnetic fabric. Changes were only observed when a mound of fecal pellets at the sediment–water interface was suspended by burrowing organisms and re-deposited. In these cores, well-laminated and diffusely laminated sequences both preserve prolate fabrics, so bioturbation is unlikely to be responsible for the anomalous magnetic fabrics.

Instead, we hypothesize that prolate fabrics observed at the base of core OL070503 and the uppermost $\sim$ 0.8 to 2.7 m of core SL060901, core OL070502, and core OL070503, all resulted from sediment deformation during coring. Kullenberg corers are designed to maintain the piston inside the core barrel at the sediment–water interface during coring to create a pressure differential at the top of the sediment column for collection of an undisturbed core. If the piston accelerates upwards instead of remaining at the sediment–water interface, then the sediment is pulled upwards within the barrel (McCoy 1985). Cable recoil is responsible for upward piston motion because the winch cable is attached directly to the piston (Buckley et al. 1994; Skinner and McCave 2003). Vertically laminated mud at the base of core OL070503 is a classic example of a "flow-in" section that developed during coring. This "flow-in" formed as sediment was drawn into the coring pipe by the suction generated by the piston, and resulted in a visible vertically oriented sediment fabric that distinguishes the "flow-in" from surrounding, undisturbed, horizontally laminated sediment. Kent and Lowrie (1975) point out that prolate fabrics with nearly vertical K_1 axes are commonly found within "flow-in" sections near the bottom of cores, similar to that of core OL070503.

Visually identifying the effects of deformation as a result of piston core collection can be extremely difficult, especially when the deformation is too subtle to have destroyed the sedimentary fabric or if the sediment is massive and cannot reveal macroscopic evidence for deformation. Vertical re-alignment of sediment during inflow through the core tip may not destroy the stratigraphic integrity of the core, but may significantly impact the AMS (Thouveny et al. 2000; Skinner and McCave 2003). For these situations, researchers utilize the increase in the dispersion of K_3 axes and shift in K_3 orientations from vertical to nearly horizontal (Rosenbaum et al. 2000), a corresponding shift in the orientation of K_1 axes from nearly horizontal to almost vertical (Thouveny et al. 2000), and the gradual transition from oblate to prolate magnetic fabrics upcore, to identify the transition from normally compacted sediments near the base of the core to vertically strained sediments near the core top (Thouveny et al. 2000; Skinner and McCave 2003). Based on this work, we hypothesize that mid-core "flow-ins" are responsible for the gradual transition from oblate to prolate fabrics and the shift in the inclination of K_1 and K_3 axes observed in the diffusely laminated silty clay in core SL060901 and massive silt in core OL070502 and core OL070503. The variation in the vertical extent of these mid-core "flow-ins" likely depends on the sediment water content and composition, as well as the weight of the coring apparatus, length and elasticity of the coring cable, and water depth, based on analysis of other piston cores by Buckley et al. (1994) and Skinner and McCave (2003). The scattered K_3 axes of samples with prolate fabrics shown on stereonets could reflect sediment deformation as the sediment was pulled in through the corer (ESM Fig. S3). Within these "flow-ins," the stratigraphy may be stretched (overthickened), but the stratigraphic order is preserved and could be used to infer relative changes in paleoenvironmental conditions. Overthickening, however, will produce higher apparent sedimentation rates (Skinner and McCave 2003).

Core handling is likely responsible for the prolate fabrics and sub-horizontal K_3 axes observed in the uppermost 2- to 4-cm of all cores in this study. Because the uppermost sediment layers are incohesive as a result of their higher water content, the water-laden sediment may settle and flow as the corer is retrieved and laid down horizontally for extrusion or storage (Kent and Lowrie 1975). Resettling grains can produce a prolate magnetic fabric with near horizontal K_3 values.

"Flow-ins" can be distinguished from slides by comparing the shape with the strength of the anisotropy (Fig. 8). "Flow-ins" and slides occur in two distinct fields. The magnetic fabric of the "flow-ins" is weak whereas slides have higher P' and most samples have an oblate fabric. Slides in Owasco Lake are also easily visually recognized by the distinct lithology of the slide blocks and abrupt changes in magnetic fabrics. In contrast, zones of deformation caused by coring mechanics, ranged from "flow-ins" that are easily recognized macroscopically, to subtle deformation that could be identified only using AMS.

It is possible that splitting or sub-sampling produced some of the anomalous magnetic fabrics. A few samples in core SL050508, core SL060901, and core OL070503 and several samples in core OL070502 have E–W trending K_1 and/or N–S trending K_3 axes that cluster on stereonets (Fig. 6), which Copons et al. (1997) show can occur during subsampling. However, except for core OL070502, samples with a prolate fabric do not exhibit these orientations (ESM Fig. S3). Subsampling of most of these cores likely did not impact the shape of the magnetic ellipsoid.

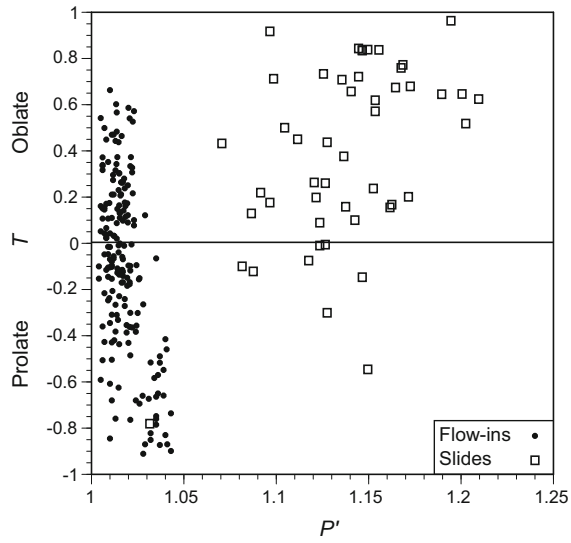

Fig. 8 The strength of the anisotropy (P') versus the shape of the anisotropy (T) for flow-in and mass movement samples from all four cores in this study

The degree of anisotropy reflects sediment compaction and an erosional unconformity associated with a lowstand

P' can be used to identify compaction and unconformities, even in sediment cores that exhibit only minor changes in lithofacies (Schwehr et al. 2006). Typically, sediments compact progressively with depth, resulting in an increase in P' (Parés 2015). Core SL060901 and core OL070503, collected from the deepest water depths, generally follow this predicted pattern, whereas core SL050508 and core OL070502, collected from shallower depths, do not (Figs. 2, 3, 4, 5). The gradual decrease in P' upcore, followed by a gradual increase in core SL050508, does not mimic the trend in % water, bulk MS, grain size, or % sand, nor does this transition reflect a change in sediment composition or lithofacies. The gradual decline in P' from 100 to 50 cm in core SL050508 records normal sediment compaction, but the abrupt increase in P' at 50 cm may demarcate the top of a zone of apparent overconsolidation. Schwehr et al. (2006) identified zones of apparent overconsolidation by comparing the expected degree of anisotropy at the same depth in other cores. They argued that core intervals with higher than expected anisotropies, given the available overburden, reflect zones where sediment was removed by erosion. Comparison of core SL050508 with core SL060901 reveals a significant difference in P' at the same core depths. At 100 cm in core SL060901, P' is 1.025, whereas at the same depth in core SL050508, P' is 1.114. Notably, P' at 100 cm in both cores collected from Owasco Lake was 1.020. The difference in P' between Seneca Lake cores suggests sediment may have been eroded, and that a disconformity may occur at $\sim$ 50 cm in core SL050508. According to Schwehr et al. (2006), a possible reason for an abrupt increase in P' is a change in sediment fabric. Below the disconformity, platy minerals may have face-to-face contacts whereas above the disconformity, they may exhibit edge-to-face contacts. In Seneca Lake, the rise in P' from 50 to 0 cm in core SL050508 may reflect the increased contribution of clay mineral abundance to the magnetic fabric (ESM Fig. S2B), and/or that an increase in alignment of these platy minerals occurred upcore. It is possible that the rise in P' at 70 cm in core OL070502 also marks a disconformity, but the disturbed magnetic fabrics (prolate) in this core interval make it difficult to interpret the trend in P' confidently (Fig. 4). Overall, P' in core OL070502 decreases upcore, but stepwise declines may reflect water content, sediment composition, and textural changes associated with changes in lithofacies.

Seismic reflection profiles and core stratigraphies record corroborating evidence for this inferred erosional unconformity. Halfman and Herrick (1998) identified wave-cut notches and an erosional surface that extends to water depths > 20 m in Seneca Lake, and Mullins and Halfman (2001) found a similar middle to late Holocene erosional surface in Owasco Lake. Additional evidence for changes in lake level comes from the geochemical and physical parameters measured in cores collected for this study. The gradual increase in %TOC, mean grain size, and % sand of the laminated mud in Seneca Lake and laminated to massive mud in Owasco Lake suggests the proximity of the littoral zone relative to the coring sites shifted lakeward by the middle Holocene. This was followed by an abrupt change in lithofacies in cores collected from Owasco Lake, from massive mud to laminated sediment, which demarcates a rise in lake level during the late Holocene. In larger, deeper Seneca Lake, a decrease in mean grain size and %TOC reflects a lake level rise. Our inferred water-level histories of Seneca Lake and Owasco Lake suggest they experienced a highstand during the early to middle Holocene, a lowstand during the middle to late Holocene, followed by another highstand. This trend generally corresponds with published lake-level histories of NY Finger Lakes. Cores collected from the modern dry valleys north or south of Canandaigua Lake, Cayuga Lake, and Owasco Lake reveal these lakes experienced maximum highstands during the early to middle Holocene and an overall gradual drying trend since the middle Holocene (Wellner and Dwyer 1996; Mullins 1998; Dwyer et al. 1996). In contrast, lakes in New England record lower-than-modern water level from $\sim$ 11 to 5.5 cal ka BP, followed by a rapid rise in lake level post-5.5 cal ka BP, and again at $\sim$ 3–2 cal ka BP (Shuman and Marsicek 2016 and references therein). Variability in the timing of lake-level fluctuations across the region may be the result of local or time-transgressive responses to climate variability (Williams et al. 2010), a shift in the dominant phase of the North Atlantic Oscillation (Menking et al. 2012) or storm tracks (Kirby et al. 2002), a paucity of radiocarbon ages and age uncertainties (Li et al. 2007),

low temporal resolution of sampling (Zhau et al. 2010), coring location within the lake basin (Lu et al. 2014), and/or isostatic rebound (Anderson and Lewis 2012). Future research will focus on analyzing a transect of cores collected from the littoral to profundal zone of these lakes that integrates additional radiocarbon dates, more paleoclimate proxies, and an isosotatic rebound model, to resolve differences in the spatial and temporal variations of inferred lake levels.

Conclusions

Combined with geochemical and physical analyses, AMS permits differentiation of primary depositional conditions from sediment disturbance associated with mass movements, erosional unconformities, and core collection. Our main findings are:

1. Subaqueous slides could be distinguished from "flow-ins" using AMS. Slides have stronger anisotropies and mainly oblate magnetic fabrics compared with non-existent to weak anisotropies and a wide range in T values preserved by "flow-ins" .
2. Mid-core "flow-ins" that did not produce obvious macroscopic sediment deformation could be recognized by a gradual change in the shape of the magnetic fabric and the orientation of K_1 and K_3 axes.
3. An abrupt increase in the degree of anisotropy was used to identify an erosional unconformity that formed during a middle to late Holocene lowstand. Coincident increases in mean grain size, % sand, and %TOC, as well as a shift in lithofacies in both lakes, all point to a drop in lake level.

Acknowledgements We thank John Halfman (Hobart and William Smith Colleges, HWS) for assistance with coring and access to high-resolution seismic reflection profiles, and Leah Joseph (Ursinus College) for assistance with AMS measurements. We acknowledge support for this work from the Keck Geology Consortium, Rochester Academy of Science (NY) and the Provost Office at HWS. Final stages of data analysis and the writing of this manuscript were completed at a workshop sponsored by NSF ADVANCE Grants 0620087 (Wesleyan University) and 0620101 (U Nebraska at Lincoln). Conversations with David Finkelstein, John Halfman, Leah Joseph, D. Brooks McKinney, and John Rayburn helped shape our ideas. We thank Stephanie Brachfield for helpful suggestions on an earlier draft and three anonymous reviewers for helpful comments and suggestions for improvement of this manuscript.

References

Anderson TW, Lewis CFM (2012) A new water-level history for Lake Ontario basin: evidence for a climate-driven early Holocene lowstand. J Paleolimnol 47:513–530

Anderson WT, Mullins HT, Ito E (1997) Stable isotope record from Seneca Lake New York: evidence for a cold paleoclimate following the Younger Dryas. Geology 25:135–138

Aubourg C, Oufi O (1999) Coring-induced magnetic fabric in piston cores from the Western Mediterranean. Proc ODP Sci Results 161:129–136

Bayliss P (1986) Quantitative analysis of sedimentary minerals by powder X-ray diffraction. Powder Diffract 1:37–39

Buckley DE, MacKinnon WG, Cranston RE, Christian HA (1994) Problems with piston core sampling: mechanical and geochemical diagnosis. Mar Geol 117:95–106

Copons R, Parés JM, Dinarès-Turel J, Bordonau J (1997) Sampling induced AMS in soft sediments: a case study in Holocene glaciolacustrine rhythmites from Lake Barrancs (Central Pyrenees, Spain). Phys Chem Earth 22:137–141

Cronin M, Tauxe L, Constable C, Selkin P, Pick T (2001) Noise in the quiet zone. Earth Planet Sci Lett 190:13–30

Dean W (1974) Determination of carbonate and organic matter in calcareous sediments sedimentary rocks by loss on ignition: comparison with other methods. J Sediment Petrol 44:242–248

Demory F, Nowaczyk NR, Witt A, Oberhnsli H (2005) High-resolution magnetostratigraphy of late quaternary sediments from Lake Baikal, Siberia: timing of intracontinental paleoclimatic responses. Global Planet Change 46:167–186

Dwyer T, Mullins HT, Good SC (1996) Paleoclimatic implications of Holocene lake-level fluctuations, Owasco Lake, New York. Geology 24:519–522

Effler SW, Perkins MG, Greer H, Johnson DL (1987) Effect of "whiting" on optical properties and turbidity in Owasco Lake, New York. Water Res Bull 23:189–196

Ellwood BB (1979) Sample shape and magnetic grain size: two possible controls on the anisotropy of magnetic susceptibility variability in deep-sea sediments. Earth Planet Sci Lett 43:309–314

Ellwood BB (1984) Bioturbation: minimal effects on the magnetic fabric of some natural and experimental sediments. Earth Planet Sci Lett 67:367–376

Ellwood BB, Hrouda F, Wagner JJ (1988) Symposia on magnetic fabrics: introductory comments. Phys Earth Planet Int 51:249–252

Frank U (2007) Paleomagnetic investigations on lake sediments from NE China: a new record of geomagnetic secular variations for the last 37 ka. Geophys J Int 169:29–40

Guiles-Ellis KG, Mullins HT, Patterson WP (2004) Deglacial to middle Holocene (16,600 to 6000 cal years B.P.) climate change in the northeastern United States inferred from multi-proxy stable isotope data, Seneca Lake. New York J Paleolimnol 31:343–361

Halfman JD, Herrick DT (1998) Mass movement of late glacial and postglacial sediments in northern Seneca Lake, New York. Northeast Geol Environ Sci 20:227–241

Hoffman J (1976) Regional metamorphism and K–Ar dating of clay minerals in cretaceous sediments of the disturbed belts of Montana. Ph.D. thesis, Case Western Reserve University, Cleveland, Ohio

Jackson ML (1969) Soil chemical analysis. ML Jackson, Madison

Jelinek V (1978) Statistical processing of anisotropy of magnetic susceptibility measured on groups of specimens. Stud Geophys Geod 22:50–62

Jelinek V (1981) Characterization to the magnetic fabric of rocks. Tectonophysics 79:T63–T67

Katari K, Tauxe L, King J (2000) A reassessment of post-depositional remanent magnetism: preliminary experiments with natural sediments. Earth Planet Sci Lett 183:147–160

Kelts K, Briegel U, Ghilardi K, Hsü KJ (1986) The limnogeology-ETH coring system. Schweiz Z Hydrol 48:104–115

Kent DV, Lowrie W (1975) On the magnetic susceptibility anisotropy of deep-sea sediment. Earth Planet Sci Lett 28:1–12

King J, Banerjee SK, Marvin J, Ozdemir O (1982) A comparison of different magnetic methods for determining the relative grain size of magnetite in natural materials: some results from lake sediments. Earth Planet Sci Lett 59:44–419

Kirby ME, Mullins HT, Patterson WP, Burnett AW (2002) Late glacial-Holocene atmospheric circulation and precipitation in the northeast United States inferred from modern calibrated stable oxygen and carbon isotopes. Geol Soc Am Bull 114:1326–1340

Lamoureux SF (1994) Embedding unfrozen lake sediments for thin section preparation. J Paleolimnol 10:141–146

Li YX, Yu Z, Kodama K (2007) Sensitive moisture response to Holocene millennial-scale climate variations in the mid-Atlantic region, USA. The Holocene 17:3–8

Lu YH, Meyers PA, Robbins JA, Eadie BJ, Hawley N, Ji KH (2014) Sensitivity of sediment geochemical proxies to coring location and corer type in a large lake: implications for paleolimnological reconstruction. Geochem Geophys Geosyst. https://doi.org/10.1002/013GC004989

McCoy FW (1985) Mid-core flow-in: implications for stretched stratigraphic sections in piston cores. J Sediment Res 55:608–610

Menking KM, Petett DM, Anderson RY (2012) Late-glacial and Holocene vegetation and climate variability. Including major droughts, in the Sky Lakes region of southeastern New York State. Palaeo Palaeo Palaeo 353:45–59

Meyers PA (2002) Evidence of mid-Holocene climate instability from variations in carbon burial in Seneca Lake, New York. J Paleolimnol 28:237–244

Michel RL, Kraemer TF (1995) Use of isotopic data to estimate water residence of the Finger Lakes, New York. J Hydrol 164:1–18

Mullins HT (1998) Holocene lake level and climate change inferred from marl stratigraphy of the Cayuga Lake basin, New York. J Sediment Res 68:569–578

Mullins HT, Halfman JD (2001) High-resolution seismic reflection evidence for middle Holocene environmental change, Owasco Lake, New York. Quat Res 55:322–331

Mullins HT, Hinchey EJ, Wellner RW, Stephens DB, Anderson WT, Dwyer TR, Hine AC (1996) Seismic stratigraphy of the finger lakes: a continental record of Heinrich event H-1 and Laurentide ice sheet instability. In: Mullins HT, Eyles N (eds) Subsurface geologic investigations of New York finger lakes: implications for quaternary deglaciation and environmental change, Special paper 311. Geological Society of America, Boulder, pp 1–36

Parés JM (2015) Sixty years of anisotropy of magnetic susceptibility in deformed sedimentary rocks. Front Earth Sci 3:4. https://doi.org/10.3389/feart.2015.00004

Rees AI (1961) The effect of water currents on the magnetic remanence and anisotropy of susceptibility of some sediments. Geophys J R Astron Soc 6:235–251

Rees AI (1965) The use of anisotropy of magnetic susceptibility in the estimation of sedimentary fabric. Sedimentology 4:257–271

Rees AI, Woodall WA (1975) The magnetic fabric of some laboratory-deposited sediments. Earth Planet Sci Lett 25:121–130

Reimer PJ, Baillie MGL, Bard E, Bayliss A, Beck JW, Blackwell PG, Bronk Ramsey C, Buck CE, Burr GS, Edwards RL, Friedrich M, Grootes PM, Guilderson TP, Hajdas I, Heaton TJ, Hogg AG, Hughen KA, Kaiser KF, Kromer B, McCormac FG, Manning SW, Reimer RW, Richards DA, Southon JR, Talamo S, Turney CSM, van der Plicht J, Weyhenmeyer CE (2009) IntCal09 and Marine09 radiocarbon age calibration curves, 0–50,000 years cal BP. Radiocarbon 51:1111–1150

Rosenbaum JG, Reynolds RL, Smoot J, Meyer R (2000) Anisotropy of magnetic susceptibility as a tool for recognizing core deformation: re-evaluation of the paleomagnetic record of Pleistocene sediments from drill hole OL-92, Owens Lake, California. Earth Planet Sci Lett 178:415–424

Sandgren P, Snowball I (2001) Application of mineral magnetic techniques to paleolimnology. In: Last WM, Smol JP (eds) Tracking environmental change using lake sediments 2. Physical and chemical techniques. Kluwer Academic Publishers, Dordrecht, pp 217–237

Schaffner WR, Oglesby RT (1978) Limnology of eight finger lakes: Hemlock, Canadice, Honeoye, Keuka, Seneca, Owasco, Skaneateles and Otisco, Lakes of New York State 1. In: Bloomfield JA (ed) Ecology of the finger lakes. Academic Press, New York, pp 313–470

Schneider JL, Pollet N, Chapron E, Wessels M, Wassmer P (2004) Signature of Rhine Valley sturzstrom dam failures in Holocene sediments of Lake Constance, Germany. Sediment Geol 169:75–91

Schwehr K, Tauxe L (2003) Characterization of soft-sediment deformation: detection of cryptoslumps using magnetic methods. Geology 31:203–206

Schwehr K, Tauxe L, Driscoll N, Lee H (2006) Detecting compaction disequilibrium with anisotropy of magnetic susceptibility. Geochem Geophys Geosyst 7:Q11002. https://doi.org/10.1029/2006GC001378

Shuman BN, Marsicek J (2016) The structure of Holocene climate change in mid-latitude North America. Quat Sci Rev 141:38–51

Skinner LC, McCave IN (2003) Analysis and modelling of gravity- and piston coring based on soil mechanics. Marine Geol 199:181–204

St-Onge G, Chapron E, Guyard H, Rochon A, Lajeunesse P, Locat J, Scott D, Stoner JS, Hillaire-Marcel C (2008) High-resolution physical and magnetic properties of rapidly deposited layers associated with landslides, earthquakes and floods. In: Locat J (ed) Geohazards. Presses de l'Université Laval, Québec, pp 119–122

Taira A, Lienert BR (1979) The comparative reliability of magnetic, photometric and microscopic methods of determining the orientation of sedimentary grains. J Sediment Petrol 40:759–772

Tarling DH, Hrouda F (1993) The magnetic anisotropy of rocks. Chapman and Hall, London

Thouveny N, Moreno E, Delanghe D, Candon L, Lancelot Y, Shackleton NJ (2000) Rock magnetic detection of distal ice-rafted debris: clue for identification of Heinrich layers on the Portuguese margin. Earth Planet Sci Lett 180:61–75

Wellner RW, Dwyer TR (1996) Late Pleistocene-Holocene lake level fluctuations and paleoclimates at Canandaigua Lake, New York. In: Mullins HT, Eyles N (eds) Subsurface geologic investigations of New York finger lakes: implications for quaternary deglaciation and environmental change, Special paper 311. Geological Society of America, Boulder, pp 65–75

Williams JH, Shuman B, Bartlein PJ, Diffenbaugh NS, Webb T III (2010) Rapid, time-transgressive, and variable responses to early Holocene midcontinental drying in North America. Geology 38:135–138

Woodrow DL, Blackburn TR, Monahan EC (1969) Geological, chemical and physical attributes of sediments in Seneca Lake, New York. Conf Great Lakes Res 121:380–396

Zhau C, Yu Z, Ito E, Zhao Y (2010) Holocene climate trend, variability, and shift documented by lacustrine stable-isotope record in the northeastern United States. Quat Sci Rev 29:1831–1843